https://doi.org/10.5194/acp-2020-47
Preprint. Discussion started: 3 February 2020

Atmospheric Chemistry and Physics Discussions

Sensitivities of the MJO Forecasts on Configurations of Physics in the ECMWF Global Model

Jun–Ichi Yano[1] and Nils P. Wedi[2]

[1]CNRM, Météo-France and CNRS, UMR 3589, 31057 Toulouse Cedex, France
[2]European Center for Medium–Range Weather Forecast, Reading, UK

Correspondence: Jun–Ichi Yano (jiy.gfder@gmail.com)

Abstract. Sensitivities of MJO forecasts to various different configurations of physics are examined with the ECMWF global model, IFS. A motivation behind this study is to explore a possibility of interpreting the MJO as a nonlinear free wave under active interactions with Rossby waves from and to higher latitudes. With this motivation in mind, various momentum dissipation terms as well as diabatic heating are selectively turned off over the tropics for the range of the latitudes 20S-20N, and it is examined how physical tendencies control the MJO dynamics. The former include eddy diffusivities as well as dissipations by both shallow and deep convection. The reduction of momentum dissipations tends to improve the MJO forecasts, but the effects are hardly additive, and their total removals rather lead to a rapid decay of the MJO, illustrating the complexity of interactions between the physics.

1 Introduction

The Madden-Julian oscillation (MJO: Zhang 2005) is a prominent tropical variability that many global atmospheric models still have difficulties in simulating. In the case of the ECMWF Integrated Forecasting System (IFS), the forecast of the propagation of the pre-existing MJO has much improved in recent years (Vitart 2014), typically providing persistent MJO signals well beyond the medium-range forecast. However, the IFS still suffers from some difficulties, especially, in predicting the onset of MJO. Needs for a capacity of extended MJO forecasts are becoming increasingly more important with increasing general interests for extended forecasts up to a subseasonal range (3–4 weeks), because the MJO is one of the most prominent and persistent tropical signals to be forecast over this time scale (*cf.*, Kim *et al.* 2018).

From an operational point of view, the MJO is typically considered physically forced in the sense that the physics in the models are the key for improving the simulation of the MJO, rather than a problem of the dynamical core (*e.g.*, Hirons *et al.* 2013a, b). The most crucial physical process to be considered is deep convection, that is typically parametrised as a subgrid-scale process in global models (Yano and Plant 2015). A majority of the existing theories for the MJO are based on a certain coupling of the large–scale dynamics with convection (*e.g.*, Hayashi 1970, Lindzen 1974, Emanuel 1987, Yano and Emanuel 1991, Majda and Stechmann 2009, Fuchs and Raymond 2017). For this reason, a general expectation is that simulations and forecasts of the MJO in the global models must be improved by improving the parametrization of deep convection (*cf.*, Jiang *et al.* 2015). The surface friction is another key process potentially expected to play a crucial role. It may be worthwhile to recall

https://doi.org/10.5194/acp-2020-47
Preprint. Discussion started: 3 February 2020


Atmospheric Chemistry and Physics Discussions

that a classical work by Chang (1977) proposes the surface friction as a key process to slow down the propagation speed of the eastward-propagating free Kelvin wave to a degree comparable to that of the MJO. The frictional wave-CISK theories by Wang (1988) and Salby *et al.* (1994) invoke frictional moisture convergence as a key ingredient in addition to deep convection for explaining the basic dynamics of the MJO.

Alternative perspectives have been proposed by Yano and Bonazzola (2009), Yano *et al.* (2009), Wedi and Smolarkiewicz (2010), Yano and Tribbia (2017), and Rostam and Zeitlin (2019), and Wang *et al.* (2019) that the tropical large–scale dynamics in general and the MJO specifically can be understood in terms of free Rossby–wave dynamics, in which model "physics" may still play a role, but secondary to the initiation and evolution. The present study investigates the implications of the MJO as a free dynamics in the context of the operational global forecasts. For this purpose, we take the ECMWF global model (IFS) as a basic framework, and perform extensive physical sensitivity experiments. The basic strategy is to turn off physical tendencies of some selective physical variables, and examine the sensitivities to the MJO forecasts. We namely consider the two variables: the momentum and the temperature (entropy).

When physical forcings are turned off from a model, an alternative mechanism for generating MJOs must also be considered. In this respect, the present study also pays particular attention to a potential importance of the interactions of the MJO with the higher-latitude dynamics. Weickmann *et al.* (1985), Knutson and Weickmann (1987) suggest that the interactions with Rossby-wave trains from and to higher latitudes are intrinsic parts of the MJO dynamics. Hsu *et al.* (1990), Gustafson and Weare (2004), Ray and Zhang (2010), Ray and Li (2013), Zhao *et al.* (2013), and Wang *et al.* (2019) further suggest that Rossby-wave trains from the northern-hemisphere higher-latitudes trigger MJOs. For investigating this aspect of the MJO dynamics, in the following sensitivity study, we attempt to simulate the higher-latitude dynamics as properly as possible in IFS. In the following sensitivity experiments, a weighting of $\cos^6\phi$ with ϕ the latitude is adopted so that the effects of the applied sensitivity rapidly tail off above $ca.$, 20°. Hence, when a certain process is turned off over the tropics, the tendency due to this process is multiplied by $1-\cos^6\phi$.

Four major categories of experiments are performed for the present study: 1) the control operational forecasts (control forecasts, or CFs), 2.a) the total physical tendency for the momentum (due to convection and the vertical eddy diffusion) is turned off, 3) all the physical tendency for the temperature (entropy) is turned off (by turning off the thermal tendency due to both shallow and deep convection parametrizations as well as all the phase changed effects associated with the microphysics), 4) all the physical tendency associated both with the momentum and the temperature are turned off. We have also performed experiments with some selective physical processes turned off associated with the momentum budget (category 2.b). Furthermore, dependence on the horizontal resolution is also investigated. However, with no strong sensitivity found by increasing from the standard resolution of 18 km further to 5 km, this aspect is not reported herein, except in Fig. 2(a) below.

Some of the key questions to be addressed are: 1) a possibility that the propagation of the MJO can be simulated even by turning off the diabatic heating due to convection; 2) a possibility that the MJO is induced by the Rossby-wave train arriving from the higher latitudes, or more specifically from an European region towards the Indian Ocean. A further question, that will only be briefly addressed, is a possibility that the MJO influences the higher-latitude circulations by radiating Rossby-wave trains towards the higher latitudes.

https://doi.org/10.5194/acp-2020-47
Preprint. Discussion started: 3 February 2020


Atmospheric Chemistry and Physics Discussions

For investigating the possibility 1), we turn off all the diabatic heating in the heat equation (entropy budget) so that an adiabatic free dynamics regime is realized over the tropics. Here, it is crucial to turn off all the diabatic heating, because if the latent heating is turned off, but the radiative cooling tendency of the tropics is maintained, a steady state can only be maintained by turning the mean ascend (associated with moist convection) to a mean descent, that induces diabatic heating that balances the radiative cooling. We turn off the total diabatic heating so that the tendency for generating any vertical motion is suppressed, and a purely horizontal, quasi-nondivergent flow is realized. Additionally turning off the momentum dissipation is expected to further enhance a tendency for a free dynamics over the tropics. For this reason, this last set-up is referred to as a quasi-free (QF) forecast in the following.

For investigating the possibility 2), we turn off the non-conservative processes (*i.e.*, frictional dissipation in general) in the horizontal momentum equation, because we expect that the free Rossby–wave dynamics associated with MJO are enhanced by turning off the momentum dissipation. As a result, we also expect that Rossby-wave interactions between the tropics and the higher latitudes are enhanced. A claim of MJO as a free Rossby wave also contains another important general implication that MJO can be principally understood in terms of the nondivergent, rotational flows. Thus, an important question to be investigated is to which extent a nondivergent (rotational) component of the MJO is still maintained by this set-up. As schematically summarized by Madden and Julian (1972, see their Fig. 16), the MJO is usually considered being strongly associated with a divergent component of the tropical circulation.

The following presentation is overall descriptive, but with a main purpose of elucidating strong sensitivities of the MJO forecasts on configurations of physics in a manner as specific as possible. Reporting the forecast performance in such specific details may even be rather unusual, but it intends to elucidate real operational issues in improving the MJO forecasts. We hope that such a thorough sensitivity investigation significantly contributes to the understanding of the basic dynamics of the MJO required for better forecasts. Specifically, we suggest the subtlety of turning off a certain physics in a given model, because nonlinearity of the system leads to various chain reactions and corresponding changes of the MJO forecast behavior. We find that a change of the results by turning off different physics hardly constitute simple additive processes, and it is likely model specific. Previous studies have found significant changes in the energy cascade behaviour of the IFS model, controlled by certain physics or specific parts thereof (Malardel and Wedi 2016). A change of the tropical processes clearly influences the interactions of the tropical processes with those in higher latitudes. Subtle balances between higher latitudes and the tropics must therefore carefully be taken into account for a full interpretation of these sensitivity results.

The following analysis is focused over the region of the Indian Ocean to the Western Pacific (90–180E), where main activities of the MJO are identified. Although the original study by Madden and Julian (1972) identifies the MJO as a global mode, as the analysis by Milliff and Madden (1996) shows, the continuous mode propagating eastwards beyond the Date Line is rather identified as a free Kelvin wave.

https://doi.org/10.5194/acp-2020-47
Preprint. Discussion started: 3 February 2020

Atmospheric Chemistry and Physics Discussions

2 Forecast Cases

2.1 General Description of the Study Period: Association of the vorticity variability with the MJO

Wedi and Smolarkiewicz (2010), Yano and Tribbia (2017), and Rostam and Zeitlin (2019) propose that the MJO is basically understood in terms of a dipolar vortex (vortex pair) symmetric to the equator. According to their theory, this vortex structure must penetrate through the whole troposphere. However in data analysis, the lower troposphere tends to be too noisy for identifying the MJO signature in the rotational wind field (or vorticity) without a proper filtering or composite procedure (*cf.*, Wang *et al.* 2019). For this reason, we focus on the 150 hPa level rotational wind field in the following. For the reasons explained in Sec. 2.4 below, we take the stream function as the diagnostic field of choice for examining the vortex dynamics associated with the MJO.

To see a clear association of the rotational wind field with the convective variability of the MJO, we show in Fig. 1(a), (b) the time-longitude section averaged over 15S-15N for the outgoing longwave radiation (OLR) and the 150 hPa stream function (with the sign flipped for the southern hemisphere so that the cyclonic vorticities are always treated as positive) for the four-month winter period (November 2016 – February 2017) from the ECMWF global analysis ("analysis" in short in the following), which is systematically adopted as an observational reference in the following. Here, data is plotted daily with the horizontal resolution of 2.5°. However, no filter is applied either in time or space. In the OLR field (Fig. 1(a)), three MJO events are identified over the Indian Ocean to the Western Pacific (90–180E) during this period: the two major ones in December and in January–February. Another weak MJO event is identified over December–January.

In association with these three MJO events, high anticyclonic activities (positive signals) over the Indian Ocean to the Western Pacific are identified (Fig. 1(b)), also propagating eastwards with a similar phase speed. From a point of view of Wedi, Smolarkiewicz, Yano, Tribbia, Rostam, and Zeitlin, these anticyclonic propagations are the key features to be simulated in association with the MJO. However, note that these propagating structures are not quite in phase, and for this reason, the absolute value for the correlation between these two fields rarely exceeds 0.3.

2.2 Model description

The IFS version cycle 43r3 (operational during 11th July 2017 - 5th June 2018) is used for the forecast experiments with (unless otherwise stated) TCo639 (average grid spacing 18 km) and with 137 vertical levels. IFS is a spectral transform model solving part of the solution in spectral space, where prognostic variables are represented via spherical harmonic basis functions. To calculate nonlinear terms in the equations of motion, to perform the nonlinear (semi-Lagrangian) advection, and to calculate the contributions of all physics schemes in grid point columns, the model fields are transformed into a representation in grid-point space. A cubic octahedral (reduced) Gaussian grid is used for this purpose, denoted by 'TCo' and described in more detail in Wedi (2014) and Malardel *et al.* (2016), typically evincing a higher effective resolution. The model is stepped forward in time using a semi-implicit time discretization for the faster (wave) processes. The model includes a realistic topography, state-of-

https://doi.org/10.5194/acp-2020-47
Preprint. Discussion started: 3 February 2020


Atmospheric Chemistry and Physics Discussions

the-art descriptions of the diabatic forcing processes, including shallow and deep convection, turbulent diffusion, radiation and five categories for the water substance (vapour, liquid, rain, ice, snow).

2.3 Choice of the forecast cases

Two forecast cases are mainly considered. Both cover one of the most prominent MJO events during the northern winter 2016–2017. The MJO in concern here corresponds to a low–skill event (F. Vitart, personal communication, March 2018) under dichotomic categorization of the MJO forecast difficulties introduced by Kim *et al.* (2016), which are more difficult than the average.

The first forecast case (called "standard" in the following: Fig. 1(c), (d)) is initiated on 19 January 2017 and run for 20 days. At this initial condition, convection associated with MJO is already fairly well developed over the Indian Ocean (Fig. 1(c)), and the key question is whether the model can maintain this convective system and also propagate eastwards as observed. From a dynamical point of view, this is before the anticyclonic vortex pair symmetric to the equator begins to develop (Fig. 1(d)). Thus the key forecast question is whether the model can predict the onset of the vortex pair.

The second cases (called "extended" in the following: Fig. 1(e), (f)) is initiated ten days earlier (9 January) than the standard case, and run for 40 days, except for the Mbb case (see below) runs for only 30 days. The initial condition corresponds towards the end of a previous MJO, and no mark of convective activity associated with the new MJO is yet to be seen over the Indian Ocean (Fig. 1(e)). Thus, a key operational challenge is to forecast the onset of convective variability associated with the MJO over the Indian Ocean. From a dynamical point of view, the vortex pair associated with the previous MJO is still well identified over the Western Pacific (Fig. 1(f)). Thus, another operational challenge is to forecast the continuous maintenance of this vortex pair, in association with a subsequent onset of another vortex pair over the Indian Ocean.

Finally, a single quasi-free forecast initiated on the 1 February 2017 is considered (QF). This is the moment that the vortex pair is fully developed over the given MJO event (Fig. 1(f)), although convection actually has already begun to fade out (Fig. 1(e)). Thus, this experiment examines whether it is possible to forecast the eastward propagation of this vortex pair even without convection.

As described in the Introduction, selective physics are turned off but only over the tropics, in the following experiments, by applying a factor, $1-\cos^6\phi$, on a physical term in concern with ϕ the latitude. The following is a list of sensitivity experiments, with forecast cases remarked in parenthesis:

1) Control forecast (CF): the same set-up as the standard control forecast in the IFS ensemble prediction system (standard, extended)

2) Sensitivity experiments on the role of the momentum dissipation (drag: M):

2.a) Turning off all the momentum dissipation (drag) tendencies in vertical eddy diffusion (including those in the boundary layer) and convection parametrization (both deep and shallow) : Ma (standard)

https://doi.org/10.5194/acp-2020-47
Preprint. Discussion started: 3 February 2020


Atmospheric Chemistry and Physics Discussions

2.b) Selectively turning off the momentum dissipation (drag) effects. The momentum tendencies for the following set of physics are turned off:

i) the whole vertical eddy diffusion: Mbe (standard)

ii) vertical eddy diffusion only in the boundary layer (below 800 hPa): Mbb (standard, extended for 30 days) :

iii) the whole convective friction: Mbc (standard)

vi) deep convective friction: Mbd (standard)

v) shallow convective friction: Mbs (standard, extended)

vi) deep convective friction and the boundary-layer eddy diffusion: Mbde (standard)

vii) shallow convective friction and the boundary-layer eddy diffusion: Mbse (standard)

3) no diabatic heating (radiation, convection, and cloud physics) : NQ (standard)

4) quasi-free dynamics case: both the whole momentum dissipation and diabatic heating are turned off: QF (standard, extended, 20 day forecast from 1 February)

Though not considered in the following, except in Fig. 2(a), two 5–6 km resolution standard forecasts are also performed:

Without deep convection parametrization : H1

No momentum dissipation (drag): H2

2.4 Analysis Procedure

2.4.1 OLR

We take the outgoing-wave radiation (OLR) as a representative of the convective variability as typically considered in the literature. Here, however, special considerations are required with this variable, because within IFS, the longwave radiation (tagged as the "top net thermal radiation" J/m^2) is recorded as accumulated values. As a standard procedure at ECMWF, the emission rate is estimated from the accumulated values as a tendency over 24 hours. Since the outgoing longwave radiation is not a one of the initialization fields, it is not included as an analysis field, either. As a result, "observational" OLR is, instead, estimated from the first 24-hour tendency of the operational daily forecasts. For this reason, even the initial 24-hour correlation is noticeably less than the unity in the following presentations (Fig. 2(a) below). The OLR anomaly is defined as a deviation from the climatology. Here, the climatology is defined as an average over the years 1979–2009 for each given calendar day.

https://doi.org/10.5194/acp-2020-47
Preprint. Discussion started: 3 February 2020


Atmospheric Chemistry and Physics Discussions

2.4.2 Vorticity field

For examining an association of MJO with the vorticity field, *or* rotational flow, we take the 150–hPa stream function. In preliminary analyses, we have also examined the vorticity field directly. However, this field turns out to be rather "noisy", being dominated by smaller scales over the tropical region with the forecast correlation typically lost more than 60 % over a single day. For this reason, we judge the vorticity field is rather an unreliable variable to predict over the tropics. The stream–function field is more predictable, being obtained by applying an inverse-Laplacian to the vorticity, and by the nature of this inverse operator, this field is much smoother. We focus on the tropopause level (150 hPa), because as it turns out, at this level, a coherent rotational flow field associated with the MJO is much easier to identify than the lower levels (*cf.*, Wang *et al.* 2018).

3 Analysis Results

3.1 Summary of forecast experiments: the correlation analyses

The time series of correlations between the forecasts and the analysis in Fig. 2 summarize the experiment results. Here, the correlation is taken over the longitudinal range of 0-180E between 15S and 15N. The anomaly field is considered for the statistics of the OLR, whereas the zonal mean is taken out from the 150–hPa stream function. A first step of verifying the performance of the sensitivity experiments would be to examine how well the convective variability associated with the MJO is predicted by these experiments. The correlations between the simulated OLR and the analysis are shown in Fig. 2(a). The same is shown in Fig. 2(b) for the rotational–wind field (150–hPa stream function). Fig. 2(c) is the same as Fig. 2(b), but focuses on the role of convective frictions (*cf.*, Sec. 3.3.2 below). Fig. 2(a) shows that higher-resolution runs with average grid-spacing of 5-6 km (H1, H2) do not dramatically perform any better than other runs, thus are not considered in the remainder of the paper.

3.2 Control Forecasts (CFs)

3.2.1 Standard 20–Day Control Forecast

With the standard 20-day control forecast (CF), the initial 0.7 correlation of OLR with the analysis linearly decreases to 0.5 approximately at the end of the forecast (short black curve in Fig. 2(a)). Inspection of the time-longitude section (Fig. 3(a)) reveals that although the convective variability is persistent in the simulation, it is too stationary (lack of propagation), and as a result it loses a correlation with the analysis with time (*cf.*, Fig. 1(c)).

The standard CF presents a rather high correlation of the 150–hPa stream-function with the analysis above 0.8 for the first 16 days (long black curve in Fig. 2(b), (c)). However, this high correlation turns out to be rather misleading, because a direct inspection of the time-longitude plot (Fig. 3(b)) reveals that the predicted stream–function signal is much weaker than analysis (Fig. 1(d)). Onset of the anticyclonic vorticity signal centered around 100E on 29 January is correctly predicted, leading to a

https://doi.org/10.5194/acp-2020-47
Preprint. Discussion started: 3 February 2020


Atmospheric Chemistry and Physics Discussions

high correlation, but with a much weaker amplitude, and the signal suddenly dies out on 4 February associated with a sudden drop of the correlation.

3.2.2 40–Day Extended Control Forecast

When the experiments are initialized 10 days earlier (9 January), the forecast is expected to be harder, because it corresponds to a final stage of the previous MJO, and a next MJO to be predicted is not yet initiated (*cf.*, Fig. 1(e)). The correlation of OLR gradually decreases to 0.4 over 20 days with CF (black curve in Fig. 2(a)). However, from this point, the correlation value begins to gradually recover, and it exceeds that of the 20-day forecast on 2 February, and increases to above 0.6 by 4 February.

Some possible interpretations are inferred from the time-longitude section (Fig. 3(c)). The last phase of the previous MJO consists of a westward propagating cloud cluster over the Western Pacific, partially driven by the linear Rossby wave dynamics. In the extended CF, this westward propagating cloud cluster continues to propagate into the Indian Ocean although it dissipates out in analysis. The continuous westward propagation effectively simulates the initiation of the new MJO, as observed. The termination of this cloud cluster on 26 January coincides with an initiation of a new cloud cluster to its east side. The new cloud cluster is also more persistent than the observed counterpart, that in turn, contributes to a significant recovery of the correlation. It is specuated that the persistence of this cloud cluster is helped by a persistent anticyclonic signal over the same region, successfully predicted albeit with a 4-day delay of onset (Fig. 3(d)), and see Sec. 3.5.2 for further discussions. The simulation predicts an initiation of another convectively active phase on 11 February, as observed. However, this convective variability turns out to be more active and persistent than observed.

3.3 Forecasts Sensitivities on Friction

Forecast performance sensitively changes by turning off some physical processes. We focus mostly on the standard 20–day forecasts first to elucidate various aspects, then briefly remark on the 40–day extended forecasts.

3.3.1 Momentum Dissipation

As it turns out, performance of the forecasts for the rotational field sensitively depends on the choice of momentum dissipation terms. This subsection discusses this overall aspect. The next subsection focuses more specifically on convective friction.

A first case to be considered is when the total tendency for the momentum dissipations (both eddy diffusive and convective: Ma) is turned off. The time-longitude section (Fig. 4(a)) shows that the eastward propagation structure of convection is better simulated than by CF. More significantly, a clear-sky area (60-70E) behind the MJO convective variability seen in the last 8 days in the analysis, but absent in CF, is successfully predicted in this case.

Turning off the vertical–eddy momentum dissipation both totally (Mbe: Fig. 4(b)) and only in the boundary layer (BL, below 800 hPa: Mbb: blue curves in Fig. 2(a) and (b); Fig. 4(c)) leads to similar results. Inspection of their time-longitude plots show that the eastward propagation tendency is better simulated by these two cases (Mbe, Mbb) than when the momentum dissipation (drag) is totally turned off (Ma: Fig. 4(a)).

https://doi.org/10.5194/acp-2020-47
Preprint. Discussion started: 3 February 2020


Atmospheric Chemistry and Physics Discussions

Inspection of the time-longitude sections of the 150–hPa stream function for those cases reveal that the anticyclonic variability associated with the MJO event is better simulated by these cases than CF: the emission of the Rossby wave energy from west during 22–28 January is suggested as a major source *e.g.*, for initiating the anticyclonic signal associated with the MJO by the time-longitude plots (Fig. 5(a) for Ma). However, the wave structure to the west of the MJO anticyclone is exaggerated compared to the analysis: it may be interpreted as a westward propagation of a free Rossby wave. A similar feature in the rotational–wind field as in Ma is also identified with the Mbb (Fig. 5(b)), but in a more intermittent manner. The forecast performance of these cases for the 150–hPa stream function in terms of the correlation is, however, not any better than the CF case as seen in Fig. 2(b).

3.3.2 Convective Friction

Turning off the convective friction tends to prolong the predictability of the MJO signal substantially as seen in the rotational wind field in Fig. 2(c) for the standard 20-day forecasts: a correlation is typically maintained at a relatively high value (*ca.*, 0.8) until the end of the forecast, in contrast to a sudden drop of the correlation with the CF (down to *ca.*, 0.4) over the last 4 days.

When the convective friction is totally turned off (Mbc: brown in Fig. 2(b)), the correlation is occasionally higher than the CF case even during the first 16 days of the forecast. Inspection of the time-longitude section (Fig. 5(c)) shows that the predicted MJO signal in rotational–wind field is also comparable to the analysis (Fig. 1(d)).

When only the shallow convective friction is turned off (Mbs: red in Fig. 2(b)), the correlation remains higher during the last phase of the forecast than when the convective friction is totally turned off. Time-longitude section (Fig. 5(d)) reveals that in this case, the anticyclone signal over 100-120E persists throughout the experiment without a break over the period of 21-27 January as observed. On the other hand, when only the deep convective friction is turned off (Mbd: blue in Fig. 2(c)), the forecast performance substantially deteriorates in the last phase. The deterioration is associated with an over-enhancement of the anticyclonic signal over the last phase (29 January to 8 February: Fig. 5(e)).

The behavior of the 150–hPa stream function when the shallow convective friction is turned off with the extended forecast (red in Fig. 2(b), Fig. 5(f): Mbs) is overall similar to that of the standard CF, except for some precursors for the anticyclonic signal leading to the new MJO event and a re-development of the anticyclonic variability towards the end of the forecast. When the boundary-layer friction further is turned off (30 days in blue, Fig. 2(b), Fig. 5(g): Mbb), the initial anticyclonic variability continues about 6 days longer than observed, and the second anticyclonic variability is also initiated 1-2 days later than observed. Its precursor, albeit weak, already has a good correlation with the analysis.

These experiments may be interpreted to suggest that turning off the momentum friction contributes to an improvement of the MJO forecast in general. However, a further removal of the momentum friction in the boundary layer (Mbde and Mbse, green and violate in Fig. 2(c), respectively) slightly reduces the forecast performance. When deep-convective and boundary-layer frictions are turned off (Fig. 5(h): Mbde), the second anticyclonic variability event is too strong, and too spread to the west. When shallow-convective and boundary-layer frictions are turned off (Fig. 5(i): Mbse), anticyclonic variabilities dramatically

https://doi.org/10.5194/acp-2020-47
Preprint. Discussion started: 3 February 2020


Atmospheric Chemistry and Physics Discussions

weaken. Especially, the second anticyclonic variability is too weak and too short: terminated 4 days before the end of the forecast.

These modifications suggest that effects of turning off the momentum dissipation are not additive, suggesting that some nonlinear interactions are going on.

3.3.3 40–Day Extended Forecasts

An initial phase of forecast of the rotational wind field (vorticity field) is easier when the experiment is initiated 10 days earlier than otherwise, because the initial condition corresponds to the maximum of the anticyclone signal (centered at 100-120E) associated with the previous MJO (Fig. 1(f)). A gradual decay of the correlation (with this anticyclonic signal) over the next 4 days is reasonably predicted by CF (Fig. 3(d)), as well as the cases without shallow convective friction (Fig. 5(f), Fig. 6(a): Mbs) as well as without boundary-layer momentum dissipation (Fig. 5(g), Fig. 6(b): Mbb).

Further analysis suggests that the 40-day extended CF simulates the rotational field associated with a MJO rather for the wrong reason: a dipolar vortex structure, constituting an analogue to analytical nonlinear *modon* solution, is formed by the northern-hemisphere anticyclone with a well–isolated cyclone further north rather than with a southern-hemisphere counterpart. The same interpretation also applies to the Mbs case.

3.4 Free–Dynamics Experiments

One of the reasons for our focus on the frictional terms in these sensitivity experiments is to test a possibility of interpreting the MJO as a free nonlinear Rossby wave as proposed by Wedi, Smolarkiewicz, Yano, Tribbia, Rostam, and Zeitlin. This subsection discusses this aspect by gradually turning–off more forcing and dissipation terms.

A first glimpse of a tendency towards the free dynamics is found, when both the total momentum friction and diabatic heating are turned off both in standard and extended forecasts cases: the OLR signal decays over the fist few days (about four days): See Fig. 6(c) for the 40–day extended forecast. Though some correlations persist beyond this point, that is achieved only by a very weak OLR signal predicted.

The case without diabatic heating (NQ) is of a particular interest, because the vortex dynamics is no longer coupled with convection, against what the standard theories presume for the MJO. Without surprise, the correlation steadily decreases with time approximately linearly to 0.2 towards the end of the forecast. The inspection of the time-longitude section of 150–hPa stream function (Fig. 7(a)) shows that the rotational wind field at this level decays fairly rapidly without diabatic heating, but leaving a small-amplitude wave field. It may be worthwhile to emphasize that the decay process of the anticyclonic signal from the previous MJO is fairly realistic in this forecast, though arguably slightly too fast. A subsequently-generated weak wave field may also be worthwhile to discuss: The cyclonic signal centered around 220-250E also amplifies realistically as observed, then it leads to a westward propagation, presumably as a free linear Rossby waves, which turns into a anticyclonic signal around 170E and continues to propagate westward. On 31 January, the anticyclonic signal arrives 100E, that contributes to a significant recovery of the correlation (*ca.*, 0.6 from *ca.*, 0.2 two days earlier).

https://doi.org/10.5194/acp-2020-47
Preprint. Discussion started: 3 February 2020


Atmospheric Chemistry and Physics Discussions

When the momentum friction is further turned off with the standard forecast (green curves in Fig. 2(a) and (b), Fig. 7(b): QF), the overall behavior of the system remains similar, but rather unintuitively (despite the lack of momentum dissipation), the westward propagating Rossby-wave signal decays much faster and the amplitude is weaker than the case without turning off the momentum friction (NQ), say, by a factor of three. As a result, the correlation with the analysis also becomes slightly smaller (by 0.1-0.2). A similar behavior is also seen with an extended run (Fig. 6(c), Fig. 7(c): QF).

A final experiment to test the idea of free MJO dynamics is initiated on 1 February 2017 (QF), when a vorticity pair associated with the MJO is already fully developed. Thus, this experiment examines whether it is possible to forecast the eastward propagation of this vortex pair even without convection. At this phase, convection is no longer very active. The quasi–free forecast of 150–hPa stream function for 20 days is shown in Fig. 7(d) along with the analysis (Fig. 7(e)). The result is rather disappointing in the sense that the vortex pair rapidly dissipates over the first few days. It suggests that the model is still not dissipationless enough as we intend. Nevertheless, a rather surprising behavior is an eastward propagation of the vortex pair as expected for nonlinear solitary Rossby waves, and opposite to a sense of propagation direction expected for linear Rossby waves. The propagation speed of this decaying vortex pair is much faster than that found in the analysis.

3.5 Initiation of MJO by Intrusion of a Rossby-Wave Train?

Some studies (Hsu *et al.* 1990, Gustafson and Weare 2004, Ray and Zhang 2010, Ray and Li 2013, Zhao *et al.* 2013, Wang *et al.* 2019) suggest that an intrusion of a Rossby-wave train from the northern hemisphere to the tropical region can initiate a MJO.

3.5.1 Standard 20–Day Forecasts

The analysis of standard 20 day forecast period finds such an example over 20-27 January, as depicted in a time-latitude section for the 150–hPa stream function averaged over 20E–60E (Fig. 8(a)): a negative stream–function signal (cyclone) arrives from 80N to 30N by taking about 5 days. An inspection of this time-latitude section gives an impression that the arrival of this signal to 30N helps to re-vitalize and sustain longer the anticyclonic signal centered at 15N. Since its easward extension is considered the MJO, it leads to an interpretation that the arrival of such a Rossby-wave train helps to initiate the anticyclonic variability (vortex pair) associated with the MJO.

However, the forecast experiments tend to not favor the above interpretation in terms of the Rossby–wave train. To see this point, the performance of the CF for the same period is, first, shown in Fig. 8(b): the arrival of the Rossby-wave train appears to enhance the anticyclone over the same longitudinal range centered at 15N to a degree more than in analysis. However, as a separate time-longitude section shows (Fig. 3(b)), the anti-cyclonic signal associated with MJO decreases faster than observed over the same period with CF.

Three additional experiments (NQ, QF, Ma) provide further insights (Figs. 8(c), (d), (e)): The first is a case with all the diabatic heating (radiation, convection, cloud physics) turned off (Fig. 8(c): NQ). The second case is with both diabatic heating and all the momentum dissipation (vertical eddy transport and convection) turned off (Fig. 8(d): QF). In both cases, the arrival

https://doi.org/10.5194/acp-2020-47
Preprint. Discussion started: 3 February 2020


Atmospheric Chemistry and Physics Discussions

of the Rossby-wave train with a cyclonic signal to the subtropics (30N) is well simulated, and the resulting cyclone signal along 30N is more persistent than in CF, and even more so than in the analysis. Presumably, the absence of the momentum dissipation helps to amplify the cyclone signal with time along 30N (QF), although it is less persistent than the case without turning off any momentum friction (NQ). In both cases, a further induction of the anticyclone signal along 15N, though identifiable, much weaker than the CF case, and it totally disappears after 3 February. Finally, when all the momentum friction is turned off, but the diabatic heating is maintained (Fig. 8(e): Ma), the cyclonic signal intruding into the subtropical region (*ca.*, 30N) from the higher latitudes becomes even weaker than in the analysis. The anticyclone anomaly is induced along 15N in a realistic manner without further amplification as with the CF case.

The predictions of the rotational field in standard 20–day forecasts are overall reasonable in patterns, but larger errors in amplitude. An impression is that the MJO dipole is less isolated than in the analysis, thus the internal (nonevanescent) wave structure leads to westward propagation (or stalled) rather than eastward.

3.5.2 40–Day Extended Forecasts

Over the extended forecast period, a well-established cyclonic signal is initially identified along 30N over the longitudinal range of 20-60E (Fig. 8(f)). This initial cyclonic feature at 30N is replaced by an intermittent, but persistent anticyclonic signal along 15N from 18 January, apparently associated with an intrusion of a anticyclonic feature form higher latitudes (80N). The persistent anticyclone, in turn, appears to be associated with the onset of a new MJO.

Though this whole sequence is intuitively difficult to forecast, the extended CF somehow manages to predict the arrival of the anticyclonic signal to 15N from higher latitudes (80N to 40N) over 15-20 January (Fig. 8(g)). However, in CF, the anticyclone signal along 15N already exist at that moment, unlike the observation. This anticyclone signal at 15N further facilitates to predict the onset of the MJO, as suggested by Fig. 3(d), albeit few days later than the analysis.

Inspection of time-longitude section plots averaged over 0-20N shows that the extended CF forecast predicts the rotational–wind field for this latitudinal range rather well. The 0-20N plots show that the (south-)eastward propagation of the wave-energy in association with the Rossby-wave train over 19-23 January is rather well depicted both by the analysis (Fig. 9(a)) and the extended CF (Fig. 9(b)). It also suggests a relative isolation of the anticyclonic vorticity centered over 100-150E helps to maintain its slow eastward propagation as observed. The corresponding plot for the standard CF (Fig. 9(c)) suggests that the two slowerly–decaying wave crests (negative and positive) west of this anticyclonic feature ostensively prevents to maintain its isolation, but leading to a rapid dispersion just over few days.

Though we do not discuss in depth here, experiments show that radiation of an anticyclonic Rossby-wave train (positive signals) to the higher latitudes initiated on 17 January over the Eastern Pacific (160–80W: Fig. 10(a)) is also equally well forecast by the extended CF (Fig. 10(b)). In contrast to the northern hemisphere, there is no clear evidence of Rossby-wave variability in the southern hemisphere interacting with the tropical variability.

https://doi.org/10.5194/acp-2020-47
Preprint. Discussion started: 3 February 2020


Atmospheric Chemistry and Physics Discussions

4 Discussions

One of the purposes of the present study has been to examine an extent that the MJO can be simulated with relatively frictionless setting, being consistent with the proposed free nonlinear Rossby–wave theory for the MJO (Wedi and Smolarkiewicz 2010, Yano and Tribbia 2017, Rostam and Zeitlin 2019, Wang *et al.* 2019). Overall results from the study is rather disappointing in this respect: when all the dissipation and forcing terms both for the momentum and the entropy are turned off, the features associated with MJO disappear rather rapidly. In the first sight, this tendency appears to rather support the frictional wave–CISK theories by Wang (1988) and Salby *et al.* (1994). However, the full interpretations of the behavior of the IFS are not straightforward, because selective turn–offs of various frictional terms, on the other hand, tend to improve the MJO forecasts.

Discussions on some specific runs would elucidate this point better: with the quasi-free 40-day extended forecast (QF: Fig. 7(c)), the pre-existing anticyclonic variability over 100-150E persists almost as long as observed (7 days), albeit with weak amplitude. A weakly eastward tendency, being consistent with the nonlinear free-wave theory, may also be noticed in this simulation. In the standard 20-day forecast case, only a reminiscence of the anticyclone signature from the previous MJO event is found around 120E initially in analysis, and this feature disappears in less than two days (Fig. 1(d)). Note that no convective variability is found at the vicinity to this longitude at the initial time of this forecast period (Fig. 1(c)). The quasi-free forecast (QF) maintains anticyclonic variability longer than in the analysis albeit with a weaker amplitude (Fig. 7(b)).

We interpret these rather subtle results with our quasi–free (QF) forecasts experiments as a demonstration of difficulties for realizing a "realistic" free–dynamics experiment. The main problem with the QF forecasts in the present study is a fact that by practically turning off "all" the physical forcings, the basic state of the model also breaks down very rapidly, thus a proper background state that may support a free–dynamics MJO is also lost very rapidly. It also follows that a free MJO mode also dissipates out very rapidly. A more appropriate manner of performing free–dynamics experiments would be to maintain a background state with full physics in place, but to introduce quasi-free dynamics only to a perturbation component. The basic idea of this strategy may be understood in analogy with standard perturbation analyses. However, in the present case, perturbations must be treated in a fully nonlinear manner, to be consistent with our anticipation that the MJO is a fully nonlinear construct. Such a procedure is not straightforward, but may be considered with emerging modelling infrastructure (Kühnlein *et al.* 2019).

The present study further suggests that the MJO predictability sensitively depends on the choice of the initial condition rather in an unintuitive manner, but being consistent with a clear distinction between high– and low–skill MJO events identified by Kim *et al.* (2016): longer forecasts from an earlier phase of MJO may not be harder than a shorter one from a later phase. In the present study, the standard forecasts are initiated (on 19 January) from a pre-existing MJO, whereas 40–day extended forecasts are initiated 10 days earlier towards the end of the previous MJO event. Presumably, the latter is harder to forecast the MJO evolution, especially an onset of a new MJO. However, an inspection of the time-longitude section suggests a different picture: the longer 40-day extended forecasts tend to regenerate the MJO signal towards the end of the experiments, and the recover the forecast capacity. In some cases, their performance becomes even better than the shorter standard 20–day forecasts initiated 10 days later in terms of the correlations of the OLR and the 150–hPa stream function.

https://doi.org/10.5194/acp-2020-47
Preprint. Discussion started: 3 February 2020


Atmospheric Chemistry and Physics Discussions

As Nakazawa (1988) originally pointed out, the MJO typically constitutes a modulation of the westward-propagating cloud clusters of few-hundred km-scale. The 9 January, the initiation time of the 40-day extended forecasts, corresponds towards the end of the previous MJO event, and also a moment that the last cloud-cluster over the Western Pacific begins to propagate westwards, that marks the end of this MJO event. In the 40–day extended CF, this westward-propagating cloud cluster does not die out as observed, but continues to propagate westwards to the Indian Ocean, which marks an initiation of a new MJO under this experiment. Though the predicted new MJO weakens out at a middle, we note a recovery of the signal towards the end of the event. These initial condition sensitivities of the MJO forecasts point to a simple fact that an onset as well as evolution of a MJO should not be considered as an isolated event, but better interpreted as a part of chain of processes in the atmosphere. It also points to an importance of better understanding detailed processes associated with the MJO, in the present case, those of the westward–propagating cloud clusters.

The present study has also elucidated active interactions of MJOs with higher–latitude Rossby–wave activities. Inspections of the latitude–time sections suggest that the performance of the MJO forecasts is, at least, partially helped by the successfully simulated interactions of the MJO with the higher-latitude Rossby waves (Rossby-wave trains). At the same time, the effects could also be deteriorating. For example, a stronger Rossby-wave train creates a more continuous wave train than observed over the Indian-Ocean and over the Maritime Continent, that may even destroy the isolation of the MJO dipole structure observed, leading to the westward dispersion of the original dipole. Extensive interactions between the MJO and the Rossby-wave trains revealed by the present study further suggest richer possibilities of processes contributing to the MJO dynamics. For example: does the Rocky mountain drag contribute to the MJO by controlling the PNA structure?

As a whole, the present study elucidates the complexity of how various physical processes affect the MJO forecasts. The MJO forecast problem is often reduced to that of deep convection. However, improvement of the MJO forecast, along with the many other forecast issues, is not a matter of fixing a single physical scheme. Rather we need to examine a forecast model as a whole with its interacting physics for achieving this goal. We have more specifically suggested subtlety of turning off a certain physics in a certain model: nonlinearity of the system leads to various chain reactions for change of the forecast behavior. As a result, change of the results by turning off different physics are hardly understood as simple additive processes. Especially, change of the tropical processes clearly influences the interactions of the tropical processes with those in higher latitudes. Subtle balances between higher latitudes and the tropics must carefully be taken into account for full interpretations of those sensitivity results. The present study demonstrates, possibly rather naively, such intricacies of the model-forecast improvement problem for the MJO, that should lead to further studies.

The present study clearly demonstrate substantial sensitivities of the dynamic evolution of the MJO on various physics, other than convection, and subtle interactions between them. Many of those physics are naturally parameterized in one way or another. We speculate that further experimentation at effective resolutions well beyond what has been chosen in this study, with a correspondingly reduced set of physical parametrisations, may perhaps lead to a substantially improved MJO description.

https://doi.org/10.5194/acp-2020-47
Preprint. Discussion started: 3 February 2020

Atmospheric Chemistry and Physics Discussions

Author contributions. Forecast experiments were performed by NPW, and the graphic analyses were mostly performed by JIY. The manuscript was developed by closely analyzing and discussing the results by the two authors

Competing interests. There is no competing interest with the present work.

Acknowledgements. Discussions with Peter Bechtold and Fredric Vitart are much appreciated. A bulk part of the work was performed when the first author was visiting ECMWF during February-March 2018.

https://doi.org/10.5194/acp-2020-47
Preprint. Discussion started: 3 February 2020

Atmospheric Chemistry and Physics Discussions

References

Chang, C. P., 1977: Viscous internal gravity waves and low-frequency oscillations in the tropics. *J. Atmos. Sci.*, **34**, 901–910.

Emanuel, K. A., 1987: An air–sea interaction model of intraseasonal oscillations in the tropics, *J. Atmos. Sci.*, **44**, 2324–2340.

Fuchs, Ž., and D. J. Raymond, 2017: A simple model of intraseasonal oscillations. *J. Adv. Model. Earth. Syst.*, **9**, 1195–1211, doi:10.1002/2017MS000963.

Gustafson, W. I., Jr., and B. C. Weare, 2004: MM5 modeling of the Madden–Julian oscillation in the Indian West Pacific Oceans: Model description and control run results. *J. Climate*, **17**, 1320–1337.

Hayashi, Y., 1970: A theory of large-scale equatorial waves generated by condensation heat and accelerating the zonal wind. *J. Met. Soc. Japan*, **48**, 140–160.

Hirons L. C., P. Inness, F. Vitart, P. Bechtold, 2013a: Understanding advances in the simulation ofintraseasonal variability in the ECMWF model. Part I: The representation of the MJO. *Q. J. R. Meteorol. Soc.*, **139**, 1417–1426. DOI:10.1002/qj.2060

Hirons L. C., P. Inness, F. Vitart, P. Bechtold, 2013b: Understanding advances in the simulation ofintraseasonal variability in the ECMWF model. Part II: The application of process-based diagnostics. *Q. J. R. Meteorol. Soc.*, **139**, 1427–1444. DOI:10.1002/qj.2059

Hsu, H.–H., B. J. Hoskins, and F.–F. Jin, 1990: The 1985/86 intraseasonal oscillation and the role of the extratropics. *J. Atmos. Sci.*, **47**, 823–839.

Jiang, X., D. E. Waliser, P. K. Xavier, J. Petch, N. P. Klingaman, S. J. Woolnough, B. Guan, G. Bellon, T. Crueger, C. DeMott, C. Hannay, H. Lin, W. Hu, D. Kim, C.–L. Lappen, M.–M Lu, H.–Y. Ma, T. Miyakawa, J. A. Ridout, S. D. Schubert, J. Scinocca, K.–H. Seo, E. Shindo, X. Song, C. Stan, W.–L. Tseng, W. Wang, T. Wu, X. Wu, K. Wyser, G. J. Zhang, and H. Zhu, 2015: Vertical structure and physical processes of the Madden–Julian oscillation: Exploring key model physics in climate simulations. *J. Geophys. Res.*, **120**, 2014JD022375.

Kim, H.-M., D. Kim, F. Vitart, V. E. Toma, J.-S. Kug, and P. J. Webster, 2016: MJO propagation across the Maritime Continent in the ECMWF Ensemble Prediction System. *J. Climate*, **29**, 3973–3988.

Kim, H., F. Vitart, and D. E. Waliser, 2018: Prediction of the Madden–Julian oscillation: A review. *J. Climate*, **31**, 9425–9443.

Knutson, T. R., and K. M. Weickmann, 1987: 30–60 day atmospheric oscillations: Composite life cycles of convection and circulation anomalies. *Mon. Wea. Rev.*, **115**, 1407–1436.

Kühnlein, C. and W. Deconinck, and R. Klein, and S. Malardel, and Z. P. Piotrowski, and P. K. Smolarkiewicz, and J. Szmelter, and N. P. Wedi, 2019: FVM 1.0: a nonhydrostatic finite-volume dynamical core for the IFS. *Geosci. Model Dev.*, **12**, 651–676.

Lindzen, R. S., 1974: Wave–CISK in the tropics. *J. Atmos. Sci.*, **31**, 156–179.

Madden, R. A., and P. R. Julian, 1972: Description of global–scale circulation cells in the tropics with a 40–50 day period. *J. Atmos. Sci.*, **29**, 1109–1123.

Majda, A. J., and S. N. Stechmann, 2009: The skeleton of tropical intraseasonal oscillations. *Proc. Natl. Acad. Sci.*, **106**, 8417–8422.

Malardel, S., and N. P. Wedi and W. Deconinck and M. Diamantakis and C. Kühnlein and G. Mozdzynski and M. Hamrud and P.K. Smolarkiewicz, 2016: A new grid for the IFS. *ECMWF Newsletter*, **146**, 23-28.

Malardel, S., and N. P. Wedi, 2016: How does subgrid-scale parametrization influence nonlinear spectral energy fluxes in global NWP models?. *J Geophys. Res*, **121**, 5395-5410.

Milliff, R. F., and R. A. Madden, 1996: The existence and vertical structure of fast, eastward-moving disturbances in the equatorial troposphere. *J. Atmos. Sci.*, **53**, 586–597.

Nakazawa, T., 1988: Tropical Super clusters within intraseasonal variations over the western Pacific. *J. Met. Soc. Japan*, **66**, 823–839.

https://doi.org/10.5194/acp-2020-47
Preprint. Discussion started: 3 February 2020

Atmospheric Chemistry and Physics Discussions

Plant, R. S., and J.-I. Yano (Eds), 2015: *Parameterization of Atmospheric Convection*, Volumes I and II, World Scientific, Singapore, Imperial College Press, London.

Ray, P., and T. Li, 2013: Relative Roles of Circumnavigating Waves and Extratropics on the MJO and Its Relationship with the Mean State. *J. Atmos. Sci.*, **70**, 876–893.

Ray, P., and C. Zhang, 2010: A case study of the mechanics of extratropical influence on the initiation of the Madden–Julian oscillation. *J. Atmos. Sci.*, **67**, 515–528.

Rostami, M., and V. Zeitlin, 2019: Eastward–moving convection–enhanced modons in shallow water in the equatorial tangent plane featured *Phys. Fluids*, **31**, 021701

Salby, M. L., R. R. Garcia, and H. H. Hendon, 1994: Planetary-scale circulations in the presence of climatological and wave-induced heating. *J. Atmos. Sci.*, **51**, 2344–2367.

Vitart, F., 2014: Evolution of ECMWF sub–seasonal forecast skill scores. *Q. J. R. Meteorol. Soc.*, **140**, 1889–1899.

Wang, B., 1988: Dynamics of tropical low frequency waves: An analysis of the moist Kelvin wave. *J. Atmos. Sci.*, **45**, 2051-2065.

Wang, D., J.–I. Yano, and Y. Lin, 2019: Madden–Julian oscillations seen in the upper–troposphere vorticity field: Interactions with Rossby–wave trains. *J. Atmos. Sci.*, **76**, 1785–1807. https://journals.ametsoc.org/doi/abs/10.1175/JAS-D-18-0172.1

Wedi, N.P., 2014: Increasing horizontal resolution in NWP and climate simulations — illusion or panacea?. *Phil. Trans. R. Soc. A*, **372**, 20130289.

Wedi, N. P., and P. K. Smolarkiewicz, 2010: A nonlinear perspective on the dynamics of the MJO: Idealized large-eddy simulations. *J. Atmos. Sci.*, **67**, 1202—1217.

Weickmann, K. M., G.R. Lussky, and J. E. Kutzbach, 1985: Intraseasonal (30–60 day) fluctuations of outgoing longwave radiation and 250 mb streamfunction during northern winter. *Mon. Wea. Rev.*, **113**, 941–961.

Yano, J.-I., and K. A. Emanuel, 1991: An improved model of the equatorial troposphere and its coupling with the stratosphere, *J. Atmos. Sci.*, **48**, 377–389.

Yano, J.-I., and M. Bonazzola, 2009: Scale analysis for the large-scale tropical atmospheric dynamics, *J. Atmos. Sci.*, **66**, 159–172.

Yano, J.–I., and J. J. Tribbia, 2017: Tropical atmospheric Madden-Julian oscillation: Strongly–nonlinear free solitary Rossby wave? *J. Atmos. Sci.*, **74**, 3473–3489.

Yano, J.-I., S. Mulet, and M. Bonazzola, 2009: Large-scale tropical atmosphere: asymptotically non-divergent?, *Tellus*, **61A**, 417–427.

Zhang, C., 2005: Madden–Julian oscillation. *Rev. Geophys*, **43**, doi:10.1029/2004RG000158.

Zhao, C., T. Li, and T. Zhou, 2013: Precursor signals and processes associated with MJO initiation over the Tropical Indian Ocean. *J. Climate*, **26**, 291–307.

https://doi.org/10.5194/acp-2020-47
Preprint. Discussion started: 3 February 2020

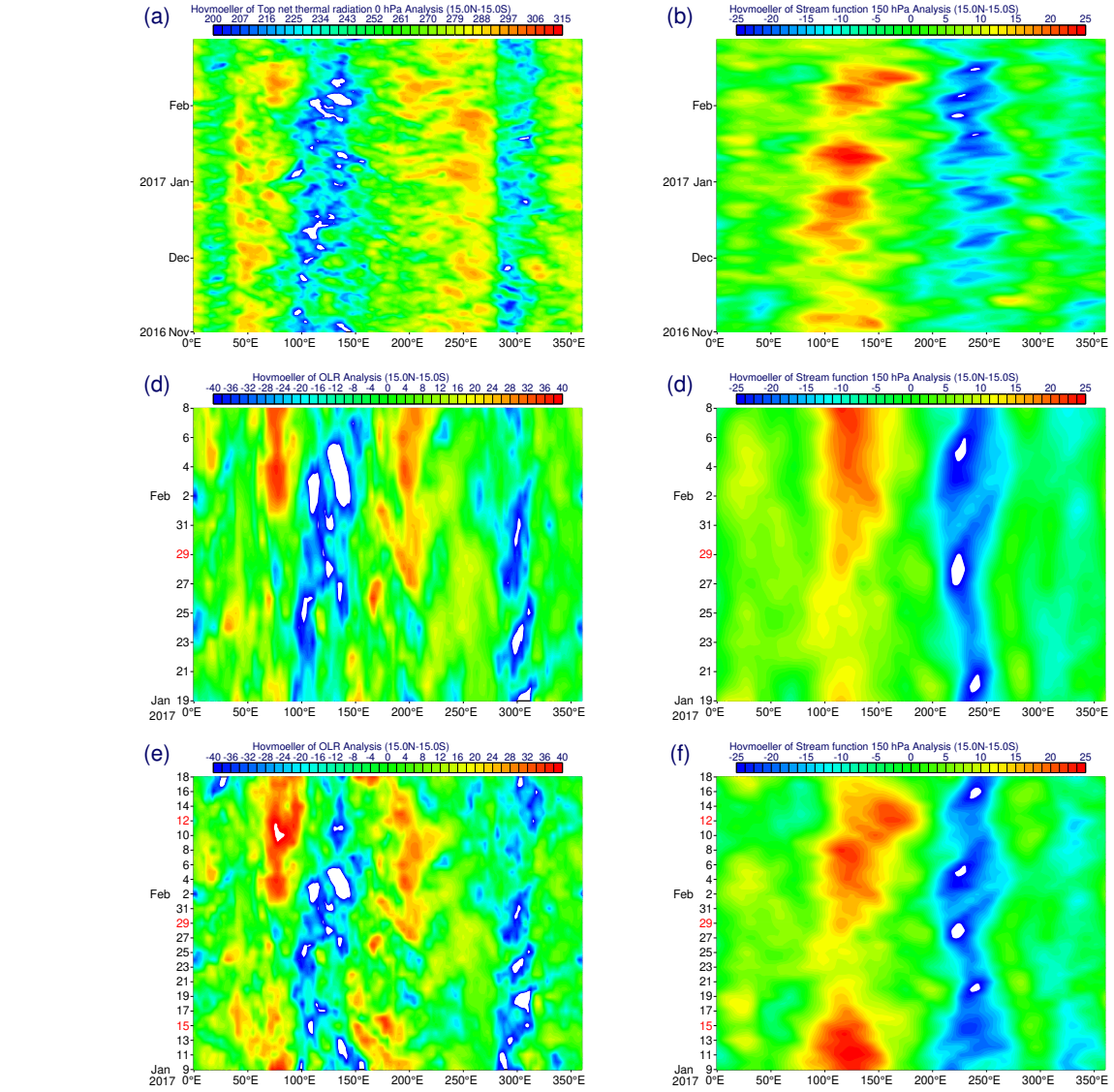

Figure 1. Time–Longitude sections averaged over 15S–15N for (a, c, e) OLR and (b, d, f) the stream function at 150hPa. Periods are for (a, b) four–month winter period of 2016–2017, (c, d) the standard 20–day forecast period, and (e, f) the 40–day extended forecast period. Anomaly fields are shown throughout here as well as in the following figures, except for the total OLR field shown in (a).

https://doi.org/10.5194/acp-2020-47
Preprint. Discussion started: 3 February 2020

Atmospheric Chemistry and Physics Discussions

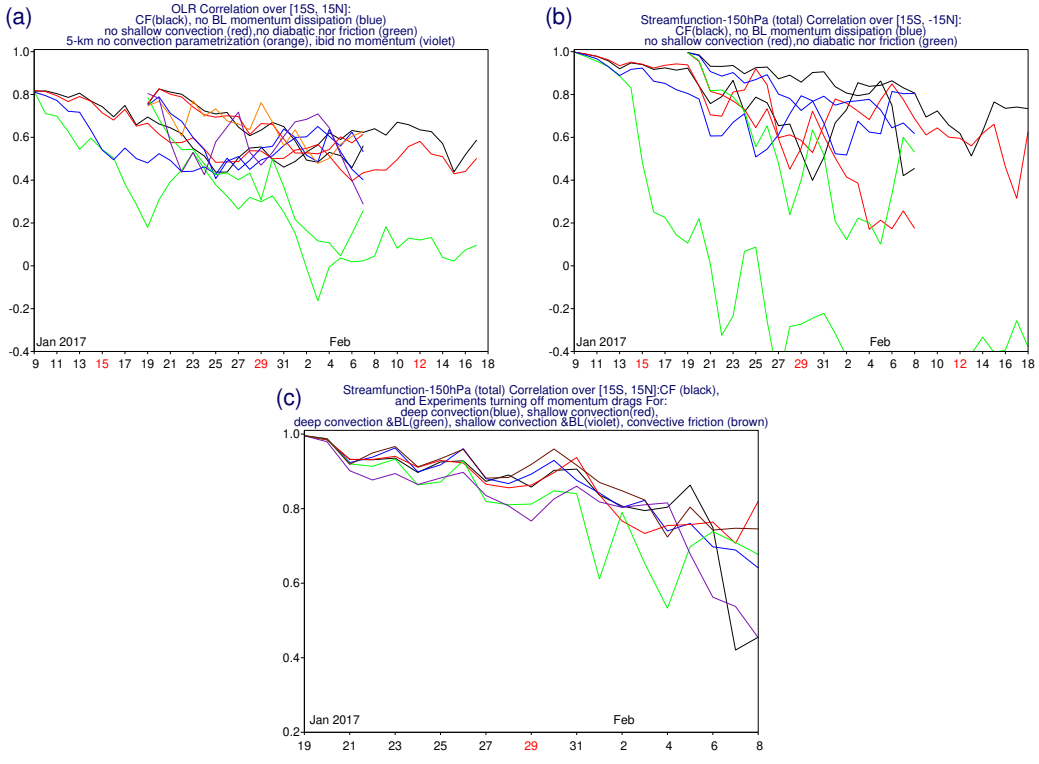

Figure 2. Time series of correlations between the forecasts and the analysis over the longitudinal bands between 15S and 15N for (a) OLR and (b, c) the 150hPa-level stream function with CFs in black curves. The other cases shown in (a, b) are for Mbb (no BL momentum dissipation: blue), Mbs (no shallow convection: red), QF (no diabatic friction: green), H1 (5-km, no convection parametrization: orange), and H2 (*ibid* with no momentum: violet) with the two last curves missing in (b). Those in (c) are for experiments turning off momentum drags for: deep convection (blue: Mbd) shallow convection (red:gwpa: Mbs), deep convection and the boundary layer (green: Mbde), shallow convection and the boundary layer (violet: Mbse), and convective friction (brown: Mbc)

https://doi.org/10.5194/acp-2020-47
Preprint. Discussion started: 3 February 2020

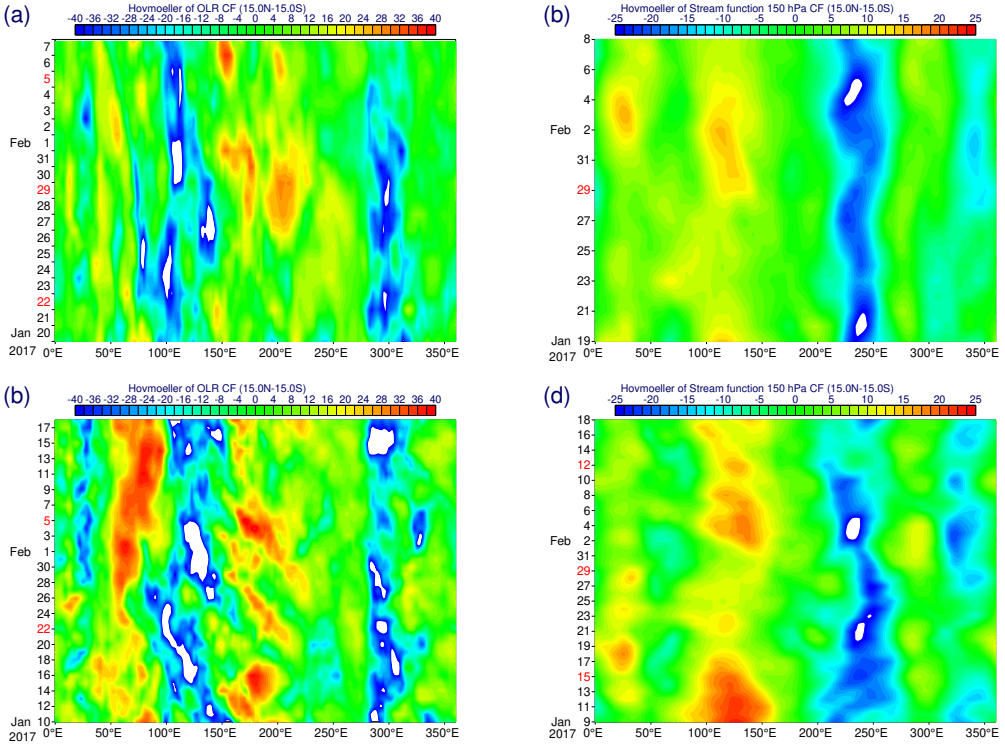

Figure 3. Time–Longitude sections averaged over 15S–15N of (a, c) OLR and (b, d) the 150hPa-level stream function for (a, b) the standard 20–day and (c, d) the 40–day extended CFs.

https://doi.org/10.5194/acp-2020-47
Preprint. Discussion started: 3 February 2020

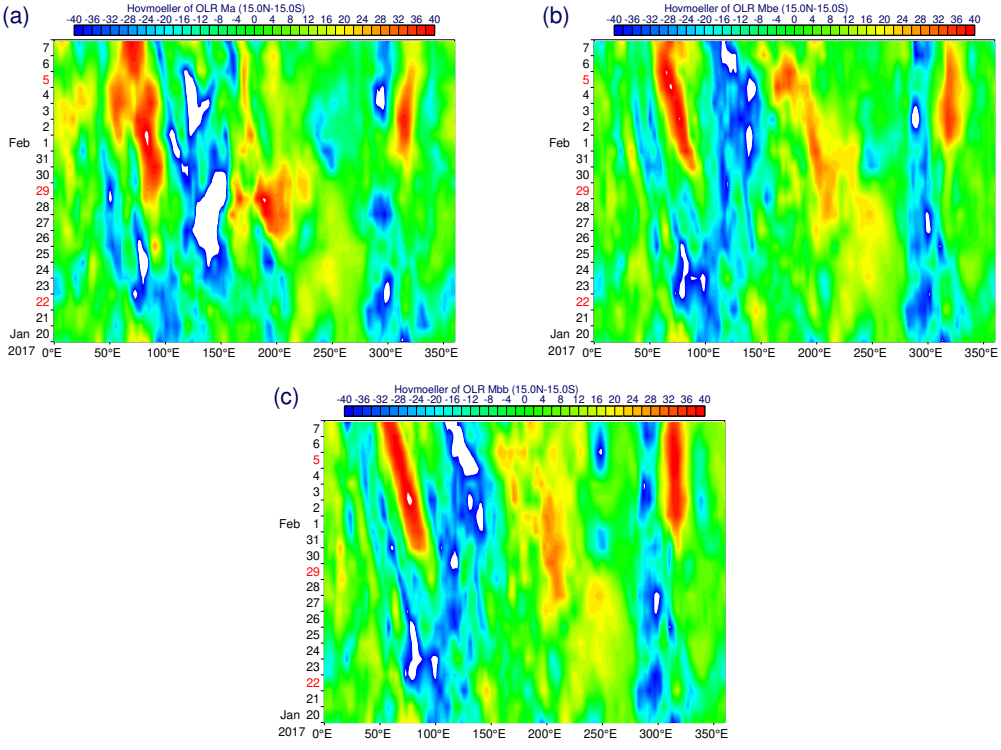

Figure 4. Time–longitude sections of OLR along the equator (15S–15N) with the the standard 20–day forecast cases: (a) Ma, (b) Mbe, and (c) Mbb.

https://doi.org/10.5194/acp-2020-47
Preprint. Discussion started: 3 February 2020

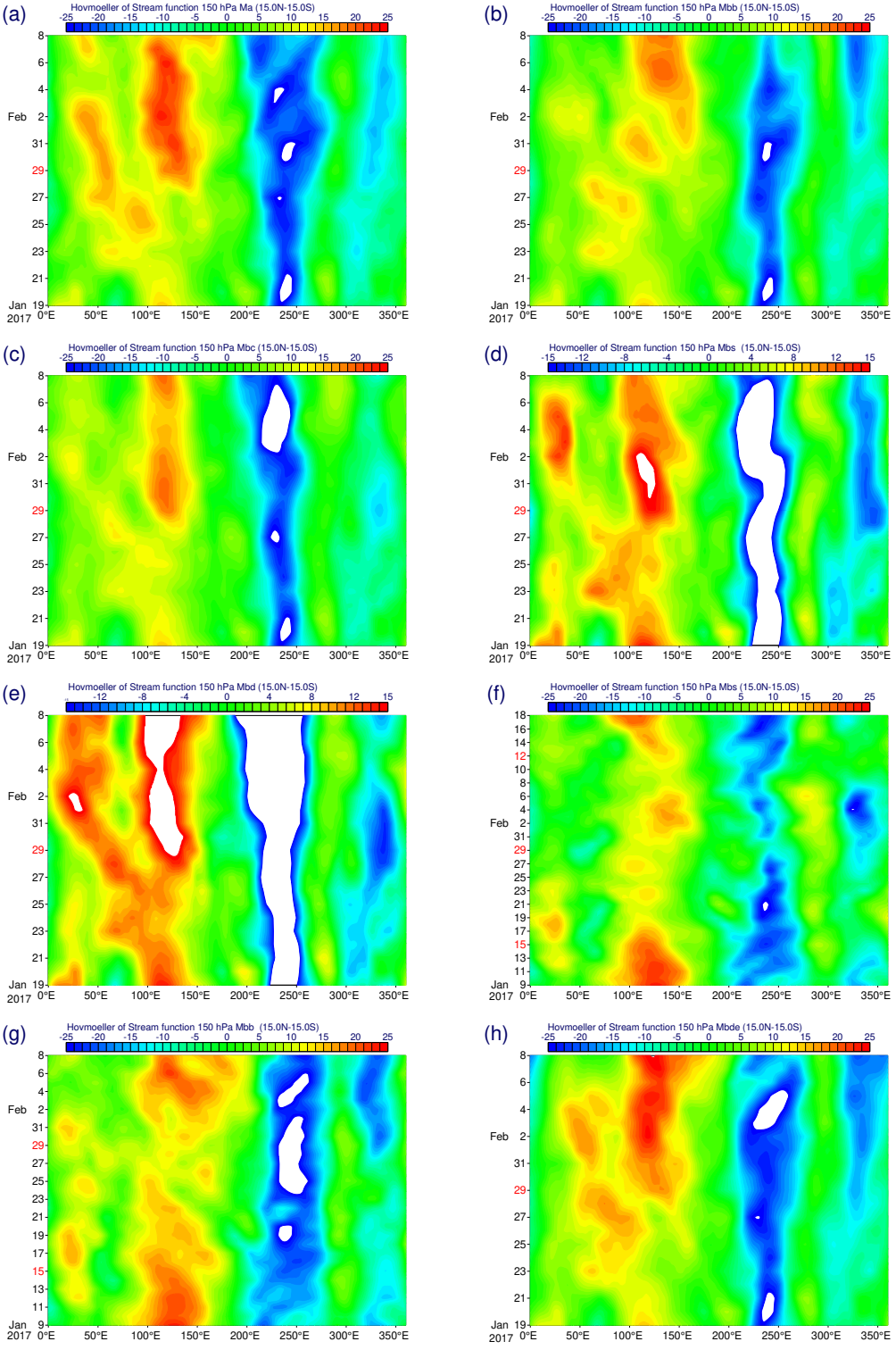

Figure 5. [See next page for the caption]

https://doi.org/10.5194/acp-2020-47
Preprint. Discussion started: 3 February 2020

Atmospheric Chemistry and Physics Discussions

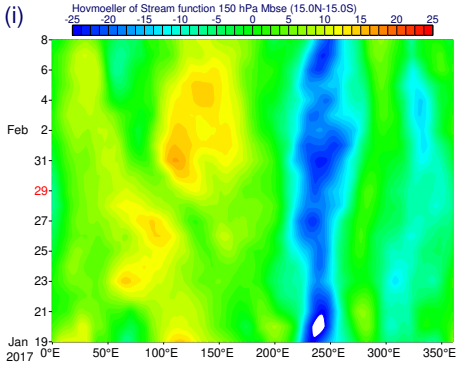

Figure. 5. Time–longitude sections of 150–hPa stream function along the equator (15S–15N) with the (a–e, h, i) standard 20–day and (f, g) extended forecast cases: (a) Ma, (b) Mbb, (c) Mbc, (d) Mbs, (e) Mbd, (f) Mbs, (g) Mbb, (h) Mbde, and (i) Mbse. Note that the Mbb case (g) exceptionally runs only for 30 days.

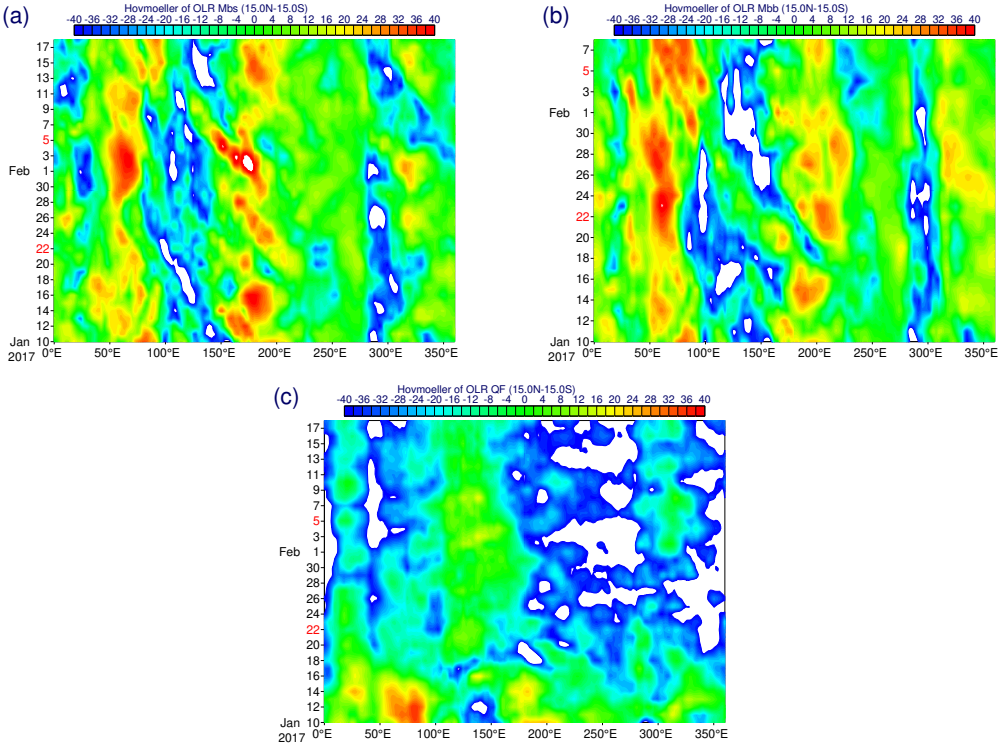

Figure 6. Time–longitude section of OLR along the equator (15S–15N) for the 40–day extended forecasts cases: (a) Mbs, (b) Mbb, and (c) QF.

https://doi.org/10.5194/acp-2020-47
Preprint. Discussion started: 3 February 2020

Atmospheric Chemistry and Physics Discussions

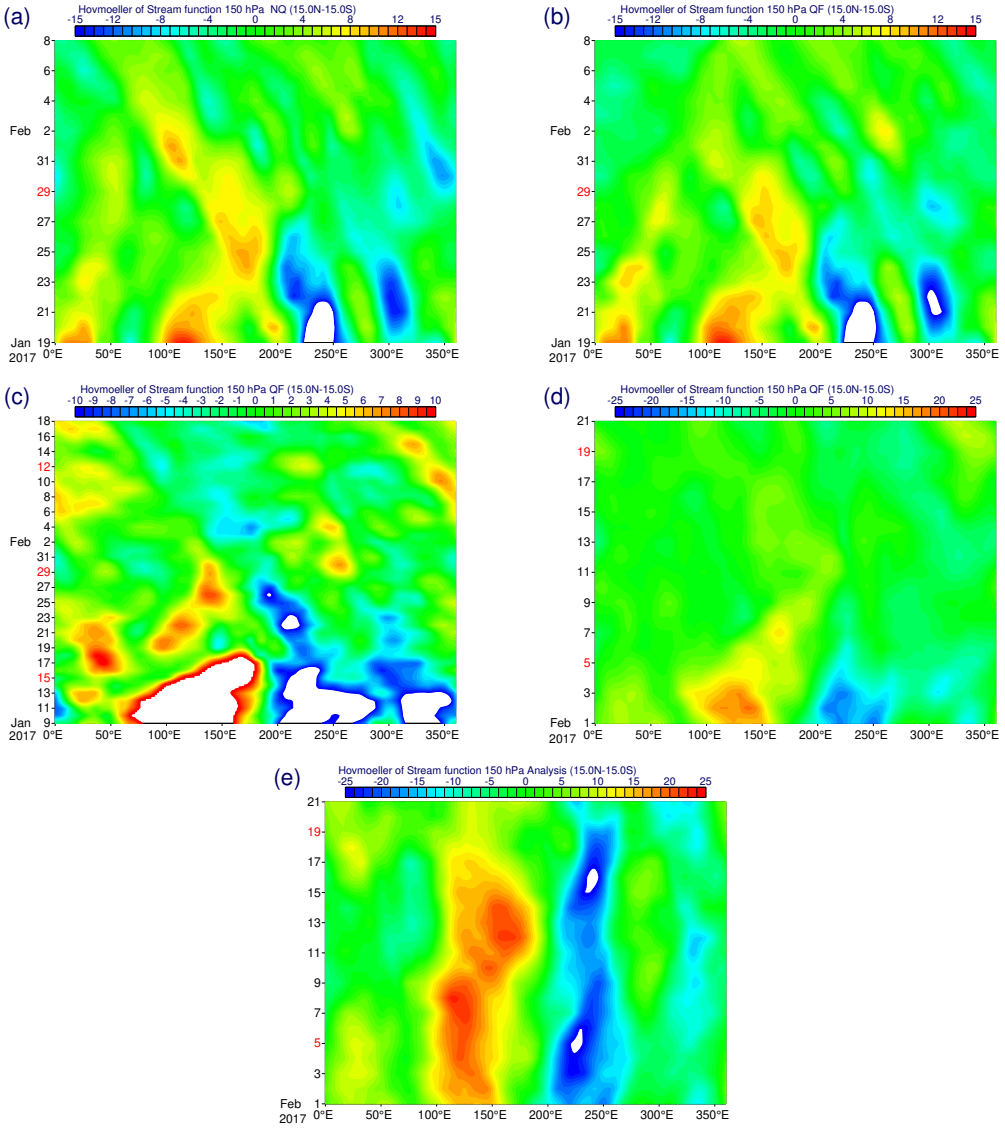

Figure 7. Time–longitude sections of 150–hPa stream function along the equator (15S–15N) with: (a) the standard NQ forecast, (b) the standard QF forecast, (c) the extended QF forecast, and (d) the 20–day QF forecast initiated on 1 February. Also shown in (e) is the analysis for the forecast period of (d).

https://doi.org/10.5194/acp-2020-47
Preprint. Discussion started: 3 February 2020

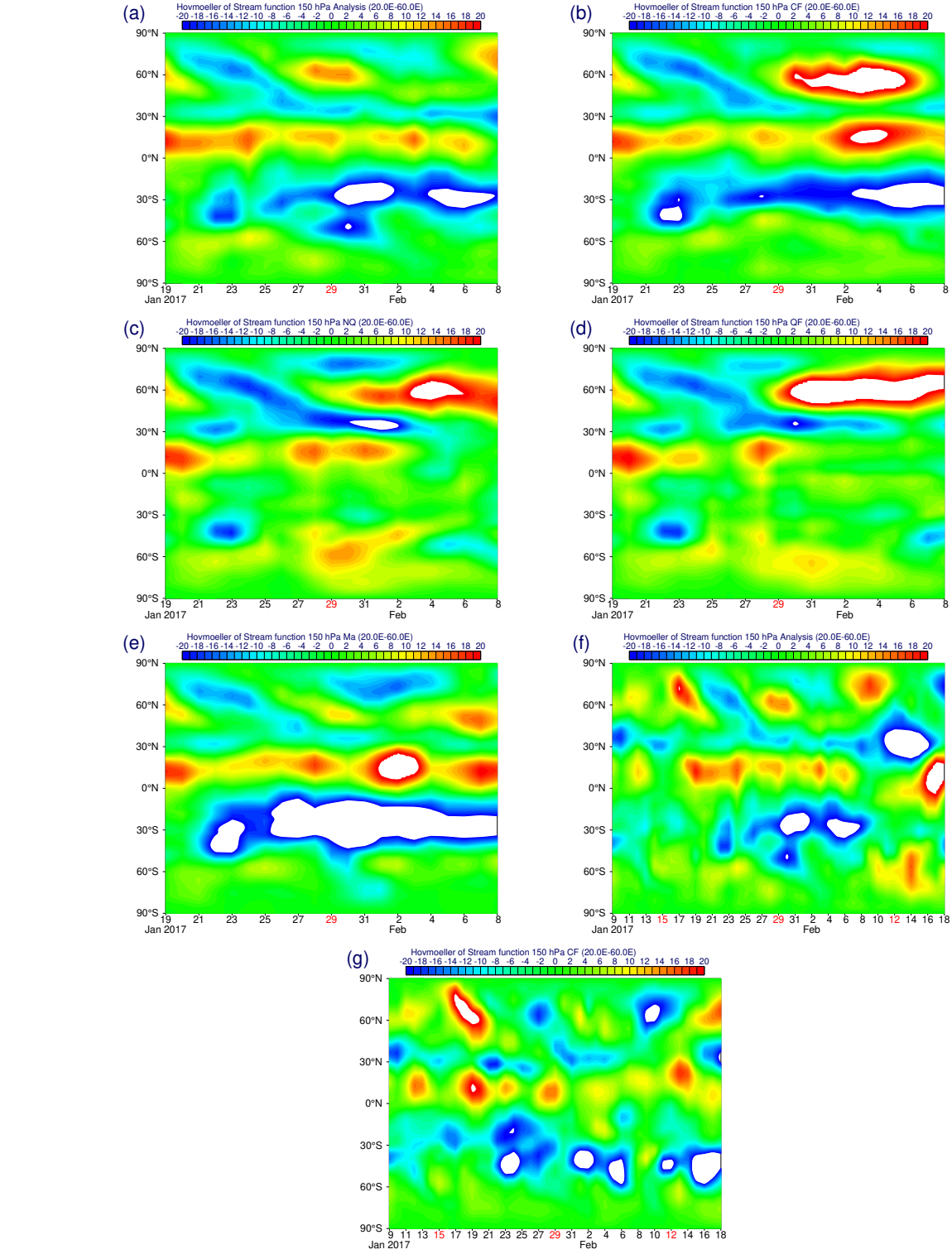

Figure 8. Time–latitude sections of 150–hPa stream function averaged over 20–60E: (a) the analysis for the standard 20–day forecast period, and standard 20–day forecasts with (b) CF, (c) NQ, (d) QF, and (e) Ma. Also for the 40–day extended forecast period: (f) the analysis, and (g) CF.

https://doi.org/10.5194/acp-2020-47
Preprint. Discussion started: 3 February 2020

Atmospheric Chemistry and Physics Discussions

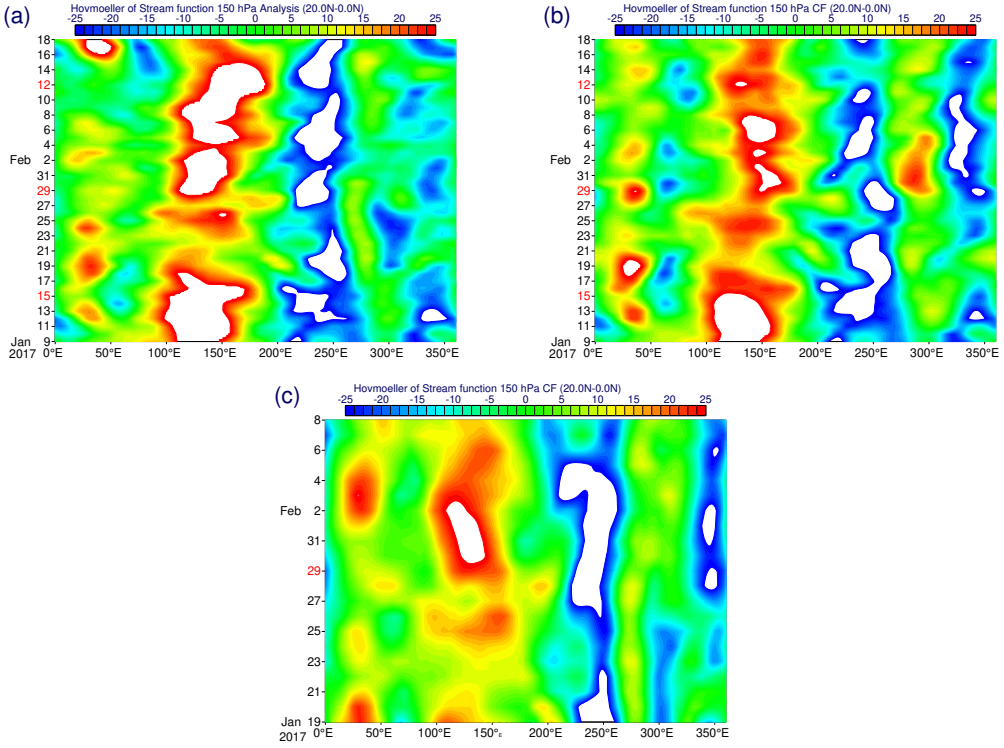

Figure 9. Time–longitude sections of 150–hPa stream function averaged over 0–20N: (a) Analysis of the 40–day extended forecast period, (b) the 40–day extended CF, and (c) the standard 20–day CF.

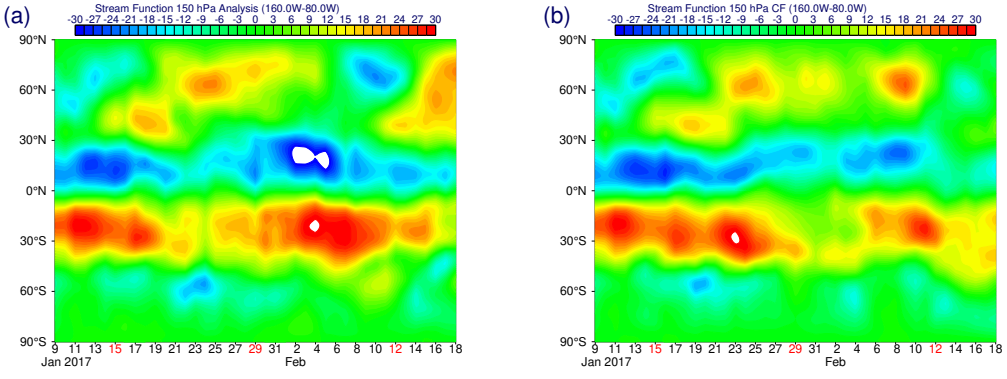

Figure 10. Time–latitude sections of 150–hPa stream function averaged over 160–80W for the standard 20–day forecast period: (a) Analysis, and (b) CF.